JOURNAL OF MATERIALS SCIENCE 31 (1996) 867–874

Precipitation in vapour quenched titanium–magnesium alloys

G. LU, P. G. PARTRIDGE, J. W. STEEDS
Department of Physics, University of Bristol, Tyndall Avenue, Bristol BS8 1TL, UK
C. M. WARD-CLOSE
Structural Materials Centre, DRA, Farnborough, Hants, GU14 6TD, UK

The effect of hot-pressing and annealing on precipitation in a Ti–9 wt % Mg alloy solid solution produced by quenching from the vapour phase is described. Precipitates about 20 nm diameter and over 100 nm diameter were found within the grains and at grain boundaries, respectively, after hot pressing at 500–600 °C. Using electron diffraction contrast imaging, selected area electron diffraction, Moiré fringe analysis and energy dispersive X-ray spectroscopy, the particles were identified as Mg. The negligible solubility of Mg in Ti led to exceptional resistance to Mg particle coarsening at temperatures up to 960 °C in the Ti beta-phase field.

1. Introduction

Although the addition of magnesium to Ti-alloys could lead to a substantial reduction in alloy density [1, 2], it is impossible to produce Ti–Mg alloys by conventional alloying techniques because of the widely different melting points and vapour pressures of the two metals and the negligible mutual solubility between Mg and Ti. However, highly supersaturated Ti–Mg solid solution alloys have been produced by a vapour mixing and quenching technique [1–3]. Complete solid solution was obtained at room temperature for compositions of up to about 20 wt % solute in both Mg-rich and Ti-rich alloys. In the as-deposited state the alloys had a columnar grain microstructure with porosity in the grain boundaries. Hot pressing converted the columnar grains to equiaxed grains. The small precipitates observed in a Ti–4 wt % Mg alloy after hot-pressing [3] were reported to increase the micro-hardness [4, 5]. This paper describes the effect of heat treatment and hot pressing on the precipitates in a Ti–9 wt % Mg alloy.

2. Experimental technique

A Ti–9 wt % Mg alloy solid solution was produced by electron beam evaporation and condensation on to a titanium substrate at 300 °C as described elsewhere [1]. The as-deposited material was about 5 mm thick and contained isolated pores in the columnar grain boundaries, which were aligned parallel to the deposit growth direction. From as-deposited material, sections for transmission electron microscopy (TEM) were cut parallel and normal to the deposit growth direction. In order to eliminate the porosity, some material was hot-pressed perpendicular to the deposit growth direction to 50% reduction in thickness under the following conditions:

1. hot-pressed at 600 °C at a strain rate of $10^{-3}\,s^{-1}$ in vacuum,
2. hot-pressed at 600 °C at a slower strain rate of $10^{-4}\,s^{-1}$ and in air,
3. hot-pressed at a lower temperature of 500 °C at a strain rate of $10^{-4}\,s^{-1}$ in air.

Specimens about $7 \times 4 \times 0.5$ mm thick were cut from the centre of the hot-pressed blocks for hardness test and TEM examination. TEM specimens were produced by electropolishing in 5% HCl, 35% 2-butoxyethanol, 60% methanol at room temperature followed by ion-milling. Imaging, diffraction and microanalysis were carried out in a Hitachi HF2000 (with a cold field emission gun) and a Philips EM-430 transmission electron microscope. *In situ* heating was carried out in the EM-430.

3. Results

The samples hot-pressed at 600 °C and strain rates of 10^{-3} and $10^{-4}\,s^{-1}$ had similar microstructures. After hot-pressing, the matrix grains became equiaxed with diameters typically about 500 nm. The porosity, which was present at the boundaries of elongated grains in the as-deposited samples, was no longer visible after hot-pressing at 500 and 600 °C. Surprisingly few dislocations were observed in these specimens, and this was attributed to rapid dislocation recovery after hot-pressing.

3.1. Identification of precipitates in Ti–Mg alloy hot-pressed at 500 and 600 °C

After pressing at 600 °C many small precipitates, about 20 nm diameter, were found within the grains. These small precipitates showed either uniform bright contrast (e.g. at B in Fig. 1a) or fringes (Fig. 1b)

0022–2461

in grains where dynamic diffraction conditions were satisfied. The precipitates were distributed inhomogeneously. For example, the area near the boundaries at X in Fig. 1a was relatively free of precipitates. The variable width of the precipitate free zones suggested they were caused by grain boundary migration sweeping up the solute atoms. There were some precipitates located at matrix grain boundaries (C in Fig. 1a). These grain boundary (GB) precipitates were usually larger than the precipitates inside grains and epitaxial with one of the grains. From large angle tilting experiments, the small precipitates were found to occur in various 3-dimensional shapes. For example with a $\langle 2\bar{1}\bar{1}0\rangle$ direction nearly parallel to the incident electron beam (Fig. 1b), the precipitates appeared in the foil plane with round (at A), ellipsoidal (at B) and hexagonal (at C) shapes, with facets parallel to the traces of the (0001) and $\{01\bar{1}0\}$ planes. The long axis of the ellipsoidal precipitates was close to the c-axis. No evidence for the formation of platelet or needle-like precipitate shapes was obtained. This indicated that the particle/matrix interface had a relatively low surface energy.

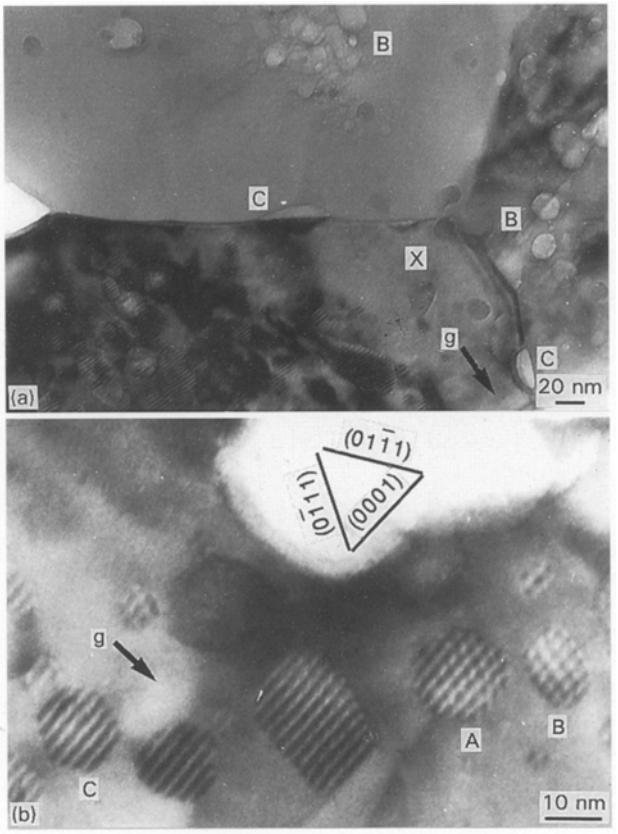

Figure 1 TEM images from a sample hot pressed at 600 °C showing (a) small particles without fringes at B, grain boundary particles at C and precipitate free zone at X, (b) small particles with fringes within grains with different shapes at A, B and C, Arrows indicate vector $\mathbf{g} = [0002]$.

X-ray energy dispersive spectroscopy (EDS) experiments showed that the small precipitates were rich in Mg (Fig. 2a) compared with the nearby matrix (Fig. 2b), where no Mg was detected. Taking a typical precipitate of 20 nm diameter embedded completely within a foil of thickness 100 nm, then the volume fraction of Ti within the irradiated volume is about 0.8 and this probably accounts for the strong Ti peak in Fig. 2a. Particles were never observed at the thin edge of the specimens, because Mg was removed by etching.

Using a thin gold film objective aperture, an equivalent aperture of about 40 nm diameter was obtained at the specimen. With the diffraction conditions used it was calculated that the effective size of the aperture was 45 nm. A selected area diffraction (SAD) pattern was taken with this diffraction aperture located over a small precipitate showing fringes and located at a distance of 50 nm from any other precipitate, as shown in Fig. 2c. The low order reflections, such as (0002) and $\{1\bar{1}01\}$, and the surrounding satellite reflections in the diffraction pattern came only from the precipitate and its surrounding matrix, respectively. The strong reflections in Fig. 2c correspond to diffraction from a $\langle 11\bar{2}0\rangle$ zone axis of the Ti matrix. The average lattice parameters obtained from measurements of the weak satellite spots in 10 SAD patterns were a good fit to values for Mg (Table I). The small precipitates were therefore identified as Mg particles epitaxial with the Ti-matrix.

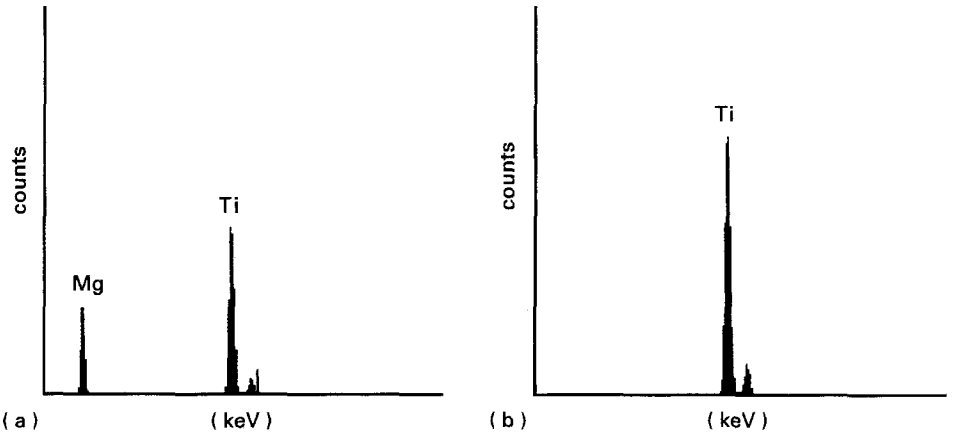

Figure 2 EDS spectra from (a) a small particle, showing high Mg, (b) the matrix showing absence of Mg, and (c) a SAD pattern near $\langle 11\bar{2}0\rangle$ zone axis. The Ti matrix diffraction spots are indexed, and the Mg satellite spots in $\langle 0001\rangle$ are marked X and those in $\langle 1\bar{1}01\rangle$ direction Y.

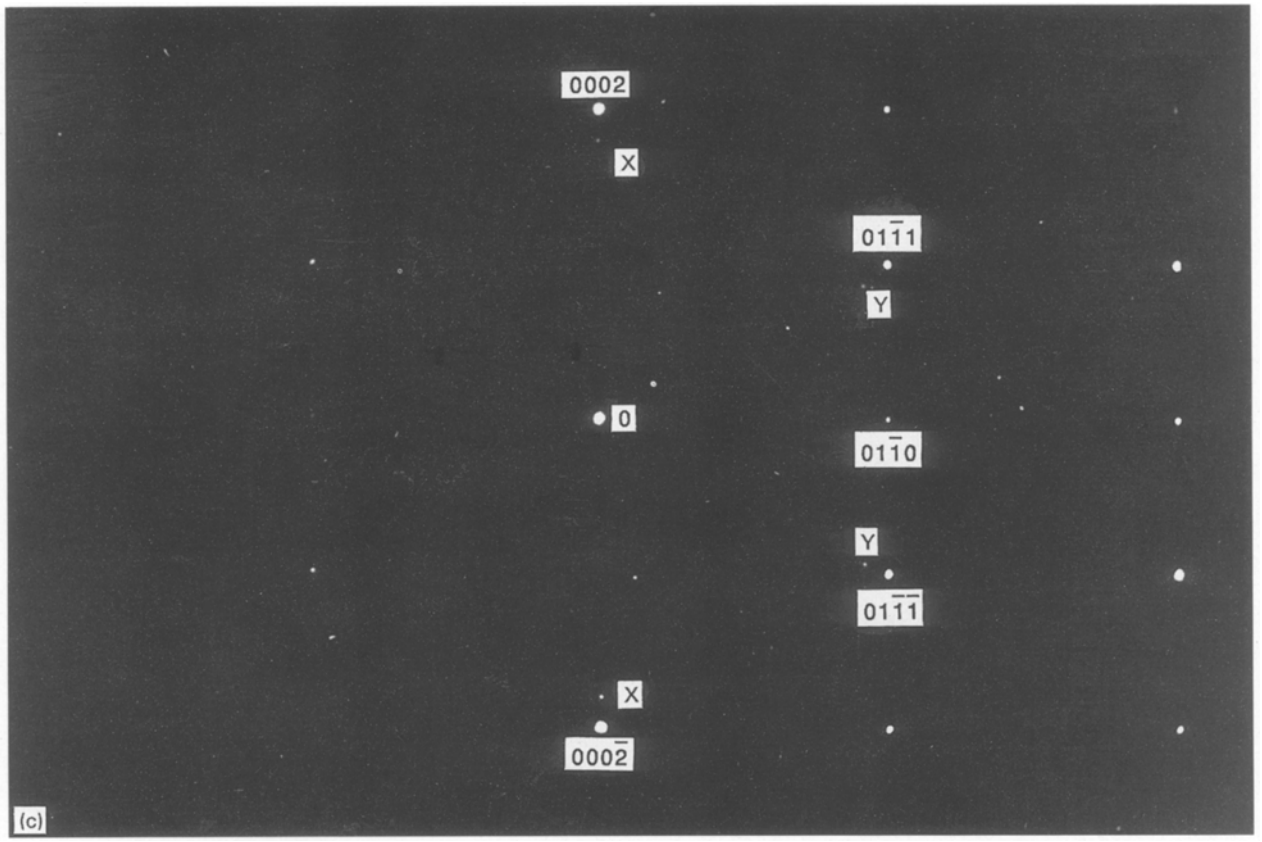

Figure 2 (Continued)

TABLE I Measured lattice parameters of the precipitate particles compared with values reported for Mg

Condition	Lattice parameters measured (nm)		Lattice parameters Mg data (nm)	
	a	*c*	*a*	*c*
Hot pressed	0.322	0.522	0.32089	0.52101
In situ annealed at 960 °C	0.320	0.520		

The Moiré fringes were also used to analyse the precipitates. These fringes are caused by interference between the matrix and precipitate reflections from planes with small differences in lattice spacings and orientation [6]. With epitaxy between the small precipitates and the matrix and with fringes in different precipitates in a grain parallel, the fringe contrast arises from the differences in lattice spacing. In the case of parallel Moiré fringes [6], their spacing D is given by $D = d_1 d_2/(d_1 - d_2)$, where d_1 and d_2 are the magnitudes of the individual plane spacings. For particle B in Fig. 1c imaged using $\mathbf{g} = [0\,0\,0\,2]$ vector near a $\langle 1\,1\,\bar{2}\,0\rangle$ zone axis, the measured average spacing between the fringes is $D = 2.27$ nm. With $d_2 = d$ (Ti, 0 0 0 2) = 0.2341 nm, the corresponding plane spacing for the precipitate is $d_1 = 0.261$ nm. Since d (Mg 0 0 0 2) = 0.2605 for pure Mg, the Moiré fringe data are consistent with the results obtained from SAD. The large GB precipitates were also identified as Mg by SAD and EDS. In some cases, the GB precipitate showed the same contrast as the small particles in one of the adjacent grains, i.e. with or without fringes depending on the diffraction conditions.

3.2. Precipitate shape and size

Moiré fringes only occur under two beam conditions (bright field) when matrix and precipitate reflections are both strongly excited. When this condition was not fulfilled the precipitate contrast was caused by differences in electron absorption, and the Mg precipitates appeared as uniformly lighter areas in the Ti matrix, as shown at B in Fig. 1a. This contrast condition was used to study the shape and distribution of nanoscale Mg precipitates. Fig. 3 shows a set of 3 bright-field images produced with a single matrix reflection, $\mathbf{g} = 1\,\bar{1}\,0\,1$, and different values for the vector $\mathbf{s}_g$, the deviation from the Bragg angle [6]. When $\mathbf{s}_g = 0$, Moiré fringes and strain field contrast obscured the images of the precipitates (Fig. 3a). With diffracted beam 7g ($\mathbf{s}_g = 0.15\ \mathrm{nm}^{-1}$) excited, a 1.2 mm underfocused image (Fig. 3b) and a focused image (Fig. 3c) was obtained. The large $\mathbf{s}_g$, underfocused image clearly shows the fringe contrast within the precipitates and the surrounding strain contrast are absent, and the precipitate shape and distribution is apparent (Fig. 3b). For example, the region arrowed in Fig. 3a is revealed as two overlapping precipitates in Fig. 3b and the dark area to the right of B in Fig. 3a, is shown to contain several precipitates in Fig. 3b. It is interesting to note the precipitate-like contrast

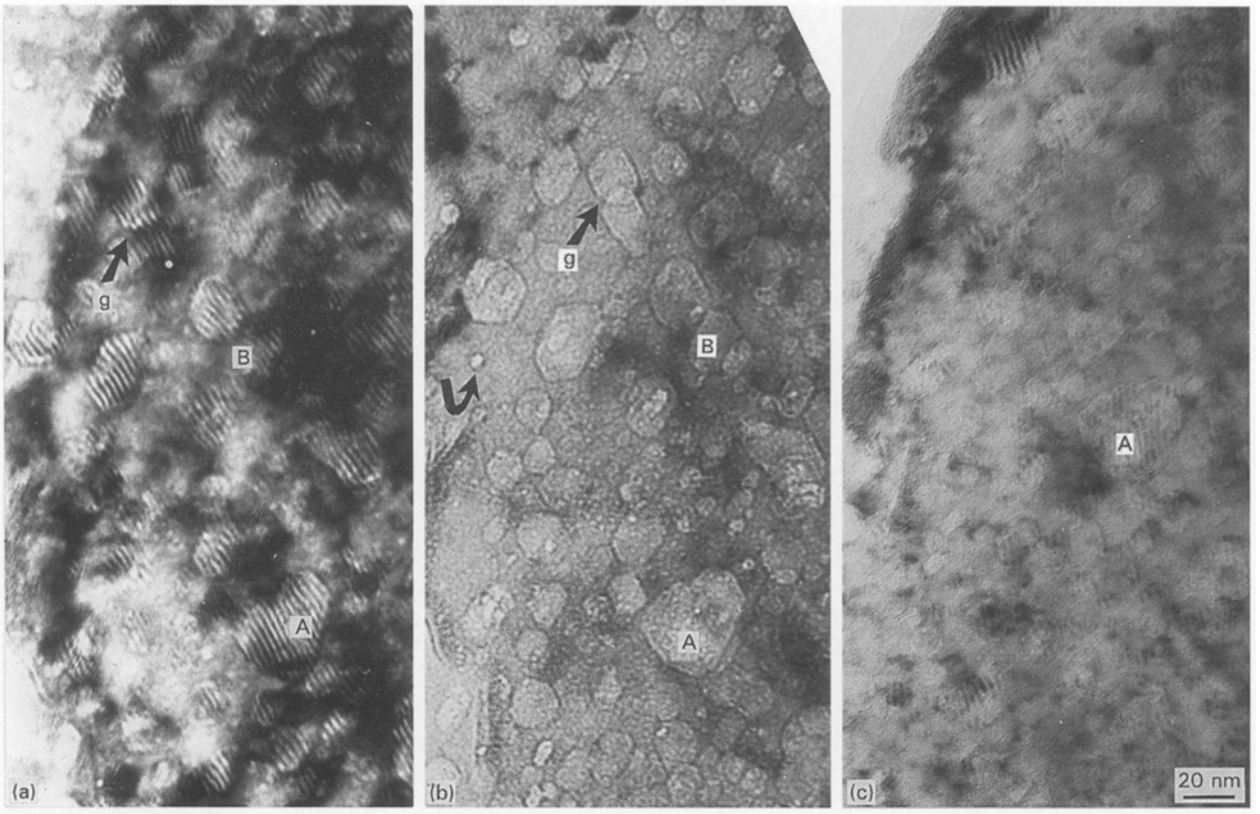

Figure 3 TEM image showing changes in contrast of the particles under different bright field two beam diffraction conditions with $\mathbf{g} = [1\,\bar{1}\,0\,1]$. (a) $\mathbf{s}_g = 0$, (b) under-focus and (c) in-focus images when diffracted beam 7g ($\mathbf{s}_g = 0.15\,\mathrm{nm}^{-1}$) is excited. Particle A is the reference point, see text.

marked in Fig. 3b with a curved arrow and verified as a Mg particle, is visible down to a diameter of about 5 nm. Below 5 nm, the identification of the precipitates by this method became problematic. Note too that the in-focus image of this region at large $\mathbf{s}_g$ (Fig. 3c) produced little contrast. Thus defocus-imaging under conditions of large $\mathbf{s}_g$ is an effective method for studying the shape and distribution of a high volume fraction of small Mg precipitates in this alloy system.

Compared with material hot pressed at 600 °C, material hot pressed at 500 °C was also free of pores and had a grain size of 500 nm (Fig. 4a), but the inter- and trans-granular Mg precipitates were fewer and smaller in size (Fig. 4b).

From the small size of the Mg precipitates and the Mg lattice parameters, it was concluded that the precipitates were incoherent, with interfacial dislocations at the interface between the precipitate and the matrix to relax the misfit strains. These dislocations were not resolved in the present experiments.

3.3. Effect of heat treatment of as-deposited samples at temperatures up to 680 °C

For comparison with the hot-pressed samples, as-deposited specimens were heated *in situ* in an electron microscope to different temperatures and held for 10 min. At 300 °C, precipitates were observed to appear occasionally. However, below 600 °C, there was very little change in the microstructure compared with the as-deposited samples. When a specimen was heated above the melting point of Mg (650 °C), many Mg precipitates were formed. An image of an as-deposited specimen after heating to 680 °C, taken under the large $\mathbf{s}_g$ defocused-image condition, is shown in Fig. 5. The precipitate size, in general, was smaller than that in the samples hot pressed at 600 °C. In this *in situ* heated sample, no massive movement of boundaries and dislocations was observed and large precipitates were absent in the grain boundaries, e.g. at A–A in Fig. 5.

Using the large $\mathbf{s}_g$ imaging technique it was possible to estimate the precipitate size and to determine the size distribution in samples heated *in situ* to 680 °C and in samples hot pressed at 500 and 600 °C. This was done by selecting a small area in a number of micrographs taken from different specimens and counting the number of precipitates that fell into a size range of $\pm$ 5 nm. Since the specimen thickness could not be determined reliably and because the precipitate size and number density changed from one area to another, the precipitate number density was normalized relative to the 5 nm precipitates and plotted against the precipitate size as shown in Fig. 6. The error due to the displacement of the first Fresnel fringe at the precipitate interface was estimated to be 1.6 nm and less than the experimental error of Fig. 6. For precipitates below 5 nm diameter, the measurements were unreliable and affected by surface oxide. From Fig. 6 it may be seen that the greatest population of precipitates occurred at 10 nm in the sample hot pressed at 500 °C and at 20 nm in the sample hot pressed at 600 °C. In the 680 °C *in situ* heated sample, more precipitates were observed in the smaller size range ($\sim$ 5 nm).

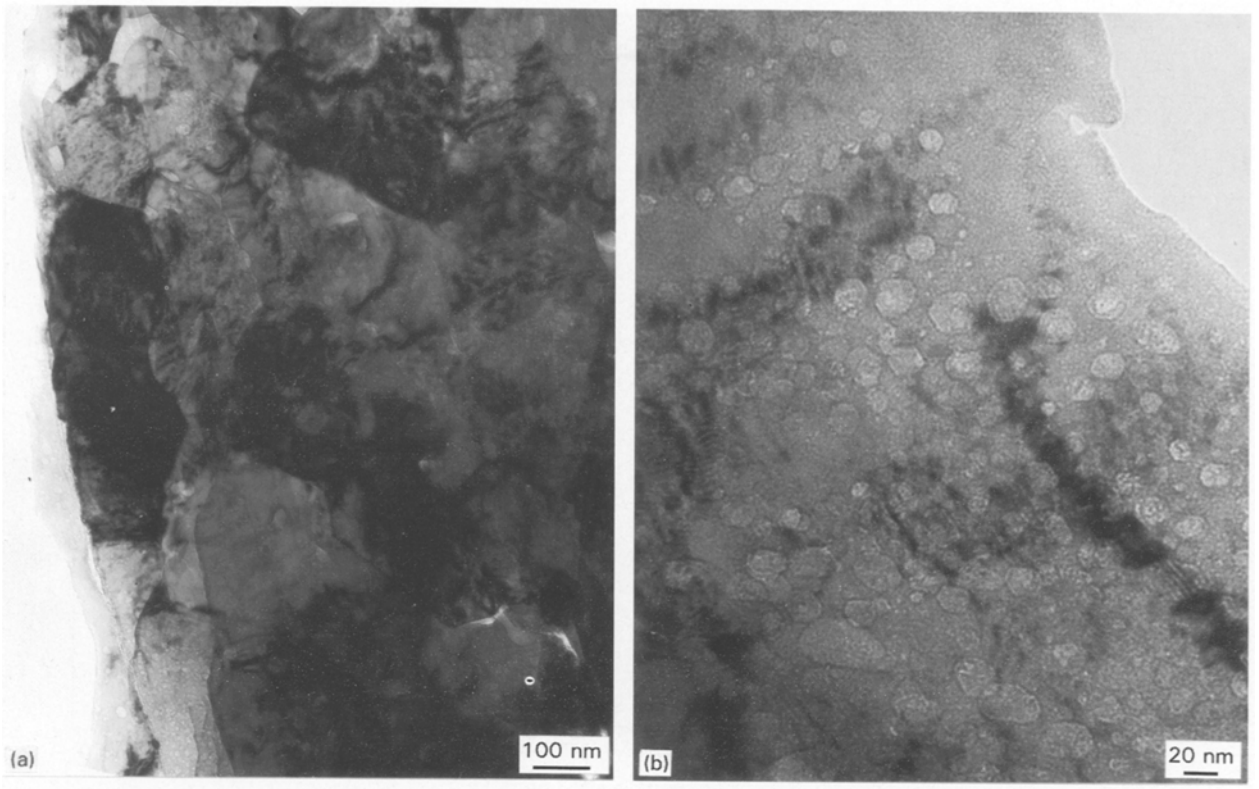

Figure 4 TEM images taken from a sample hot-pressed at 500 °C, (a) low magnification showing the grain size and (b) high magnification, showing particles inside a grain under large $\mathbf{s}_g$ defocus condition.

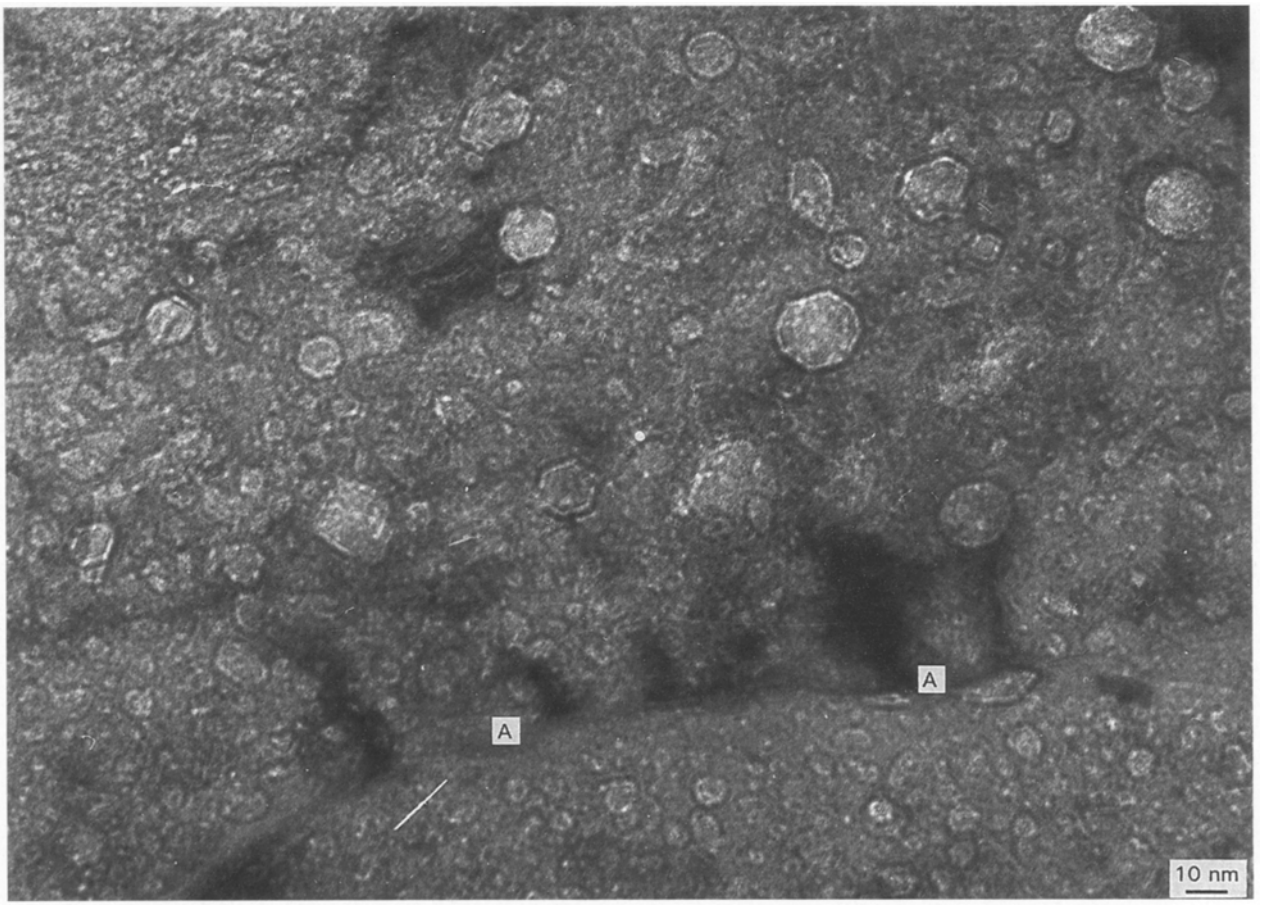

Figure 5 TEM images taken from a sample heated *in situ* to 680 °C in the electron microscope showing the particle size and number density under large $\mathbf{s}_g$ defocus condition. Note absence of large Mg precipitates in grain boundary at A–A.

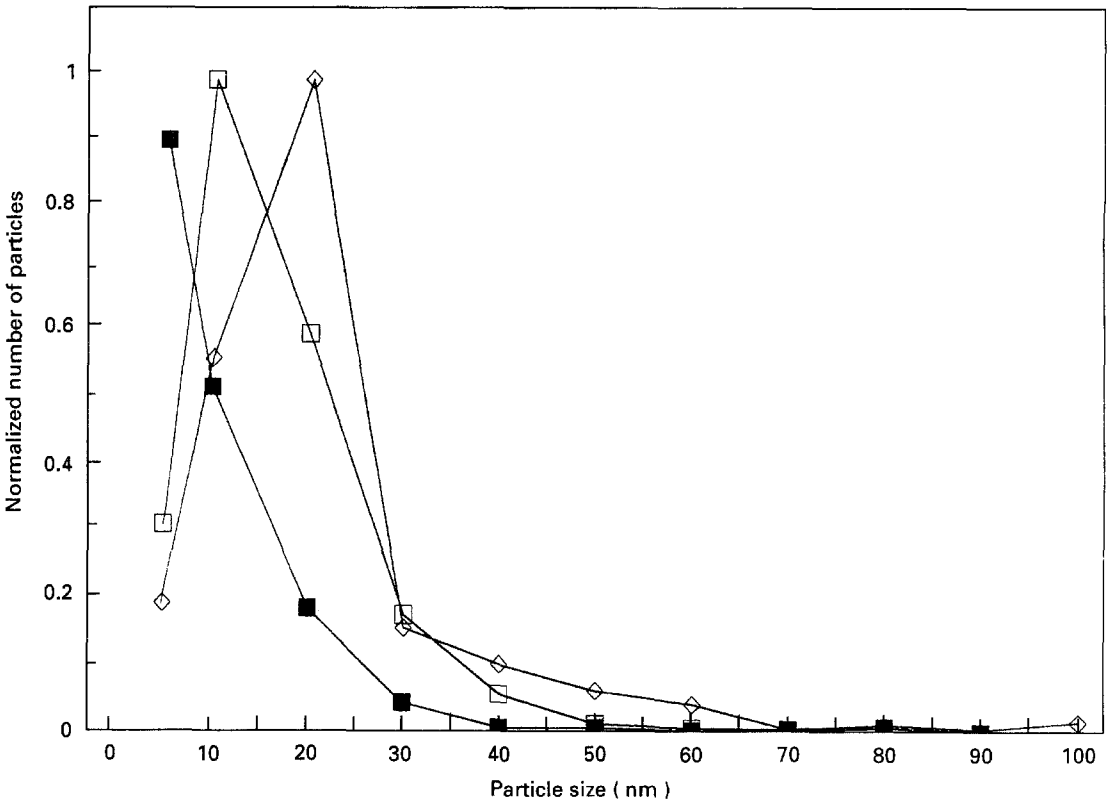

Figure 6 Normalized number of Mg precipitate particles versus particle size for hot pressed and *in situ* heated samples (◇ worked at 600 °C; □ worked at 500 °C; ■ heated at 680 °C).

3.4. Effect of heat treatment at temperatures in the range 915–960 °C

The effect of heating in the temperature range where Mg was molten and had a high vapour pressure was studied. A TEM specimen of as-deposited material was heated *in situ* in the electron microscope, to temperatures above the Ti α–β transformation temperature of 882 °C, when the crystal structure of the matrix became body centred cubic. At 915 °C some grain boundaries were seen migrating and many small circular areas of lighter contrast, "white dots", appeared of size from 10 to 100 nm (Fig. 7a). At high magnification (inset in Fig. 7a) these were identified as cavities, which intersected one of the specimen surfaces, as shown schematically in Fig. 7b. In thin areas of the foil, all the white dots were cavities. No residual Mg was detected either in the cavities or in the surrounding matrix. It was concluded that the cavities were once occupied by Mg precipitates which had evaporated at elevated temperatures. At 960 °C, the temperature was held constant for 10 min before cooling to room temperature.

In order to study regions well below the free surfaces after the above thermal treatment, thicker regions of the TEM specimen were subjected to further ion-milling to remove material from both surfaces. In these thinned regions large precipitates were observed about 1 μm in diameter located at Ti grain boundaries (e.g. A, B and C in Fig. 8a). These had lattice parameters corresponding to Mg (Table I) and EDS showed that they were rich in Mg (Fig. 8b). Also present were small round intragranular precipitates about 200 nm in diameter (at D in Fig. 8a). These small particles also contained Mg, as shown by EDS.

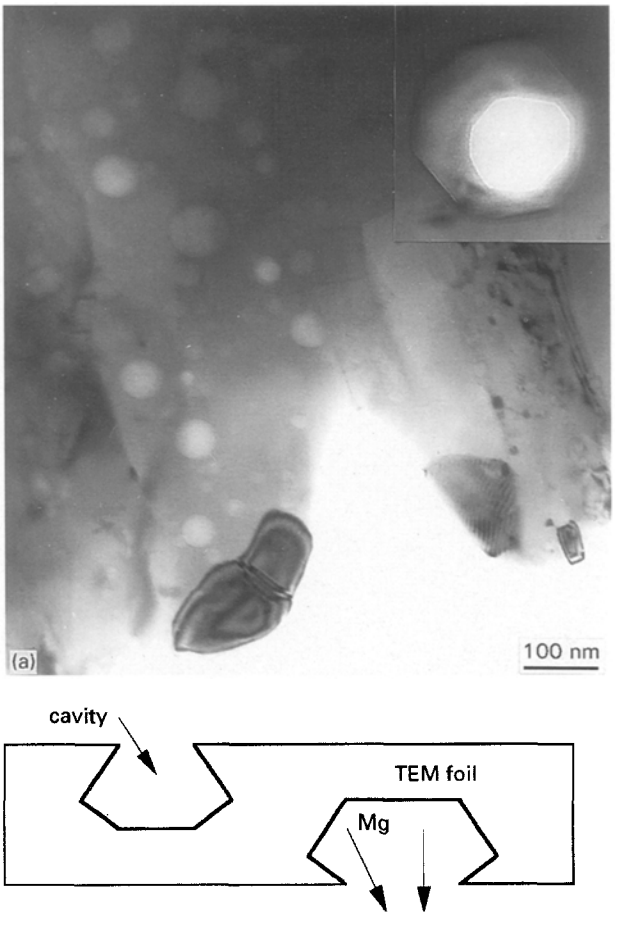

Figure 7 (a) TEM image obtained at 915 °C for an as-deposited sample heated *in situ*, showing "white dot" surface cavities which were once Mg particles. The insert shows a cavity about 40 nm in size. (b) Schematic of cavities.

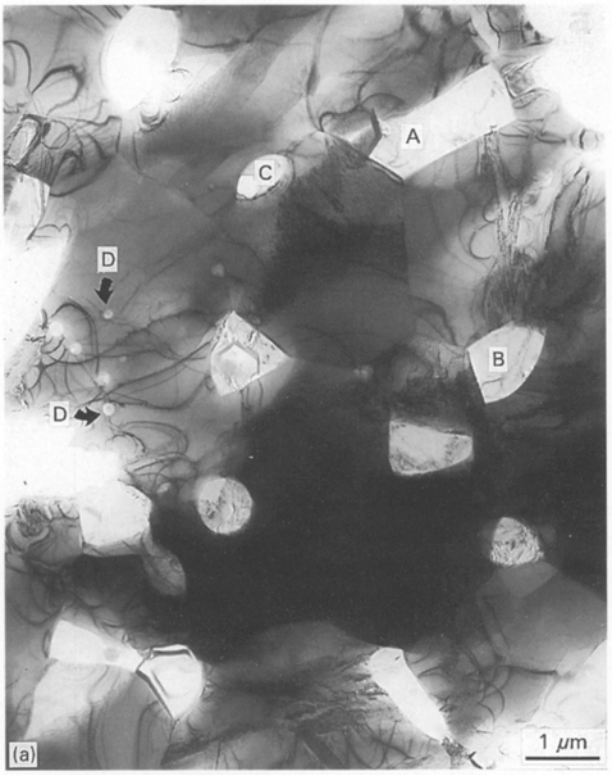

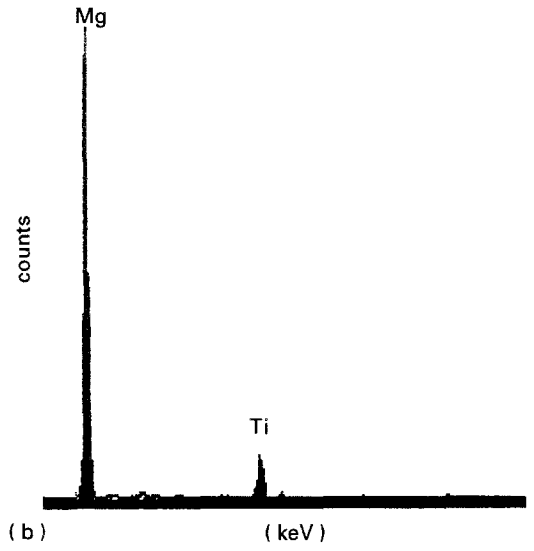

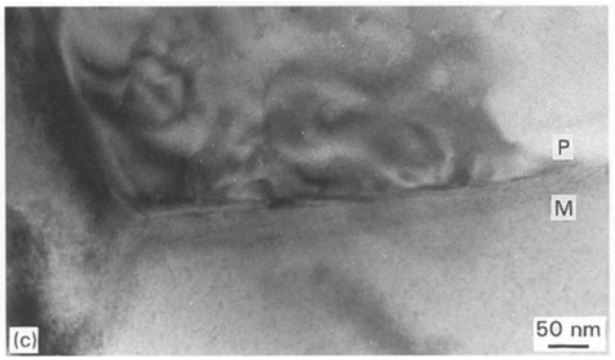

Figure 8 TEM foil heated to 960 °C for 10 min and ion-milled on both surfaces (a) large grain boundary precipitates at A, B, C and 200 nm Mg precipitates at D. (b) Typical EDS spectrum from a precipitate particles. (c) High magnification image of interface between large Mg particle P and Ti matrix M. Note continuity at the interface.

The absence of Moiré fringes indicated a lack of epitaxy with the matrix and the spherical shape is consistent with liquid or vapour phase Mg at temperature. The matrix grain size was about 5 μm.

The strain states in the large grain boundary Mg precipitates and the adjacent Ti matrix were studied using convergent beam electron diffraction (CBED). The strain in the Ti alloy had relaxed significantly after heating and recrystallization, while residual strain remained in the large Mg precipitates. This strain must have arisen after solidification of the precipitates during specimen cooling. The interface between a precipitate (marked P) and a Ti matrix grain (marked M) is shown in Fig. 8c. In spite of the particle having been well above the melting point of Mg and resolidified, and the greater thermal expansion coefficient for Mg, the interface appears continuous with the Ti matrix, with no evidence of cavities or cracks. No fixed orientation relationship was found between the Ti matrix and the large precipitates.

4. Discussion

The negligible solubility of Mg in the Ti lattice, the absence of compound formation between Ti and Mg, and the high Mg supersaturation in the alloy studied, makes Ti–Mg solid solutions unique among metastable systems studied to date. The present experiments indicate that for the first time, the study of diffusion and precipitation of Mg in hcp Ti and of diffusion in bcc Ti will be possible in these vapour quenched alloys.

The results show that as quenched Ti–9 wt % alloy solid solution is thermally stable below the melting point of Mg (650 °C) for times of ~10 min. Above the melting point of Mg at 680 °C Mg solute atoms appear to diffuse only over short distances in the lattice to form nanoscale (10 nm diameter) Mg precipitates within the grains and few grain boundary precipitates. Incoherent epitaxial Mg precipitates formed at lower temperatures during plastic deformation and recrystallization. Thus diffusion appeared to be aided by mobile grain boundaries and dislocations, and these are thought to play a major role in the formation of Mg particles during working and the loss of Mg at a free surface.

Because of the lack of solubility of Mg in Ti, the dissolution or coarsening of Mg precipitates within the grains appears to be very difficult or impossible even at temperatures above the melting temperature of Mg. Their diameters in material plastically deformed to 50% reduction in thickness at 500–600 °C or held for 10 min at 680 °C were mostly less than 30 nm diameter within grains of 0.5 μm diameter. Some Mg particles, 200 nm in diameter, were found within grains 5 μm diameter after heating to 960 °C.

Similar thermal stability was exhibited by precipitates in grain boundaries. For example the presence of many large Mg precipitates at the bcc Ti-matrix grain boundaries after 10 min at 960 °C is an indication

of the exceptional resistance to Mg diffusion in grain boundaries even when Mg is present in the liquid state with a high vapour pressure.

Further study of the mobility of Mg atoms in the solid and liquid states in Ti is now possible using this binary alloy system. The remarkable resistance to Mg diffusion apparent in the present experiments suggests interesting microstructures may be developed by hot working Ti–Mg alloys.

5. Conclusions

1. In a vapour quenched Ti–9 wt % Mg alloy all the Mg was in solid solution. The solid solution was thermally stable up to about 600 °C. Above this temperature Mg precipitates formed.

2. Plastic deformation caused Mg precipitation at lower temperatures (~500 °C). The precipitates (~20 nm diameter) within the grains were epitaxial with the matrix grains and had low interfacial energy. Larger (100 nm) Mg precipitates occurred at the grain boundaries.

3. The Mg precipitates exhibited exceptional resistance to coarsening. After heating as-quenched material to 680 °C for 10 min, a high density of 10 nm diameter Mg precipitates were present within the grains. Some 200 nm diameter Mg precipitates and 1 μm diameter Mg precipitates were found within grains and in grain boundaries, respectively, at room temperature after heating at 960 °C for 10 min within the Ti beta-phase.

4. The Mg diffusion rate in Ti appears to be extremely low, even in β-phase grain boundaries at 960 °C.

Acknowledgements

The authors would like to thank I. Farrow (Aerospace Engineering Department) and R. Vincent, D. Cherns, C. Trevor and K. E. Bagnall (Physics Department), for helpful discussions. Financial support from DRA (F) and from the Department of Trade and Industry is gratefully acknowledged.

References

1. C. M. WARD-CLOSE and P. G. PARTRIDGE, *Mater. Lett.* **11** (1991) 295.
2. C. M. WARD-CLOSE, P. G. PARTRIDGE, P. HOLDWAY and A. W. BOWEN, in "Titanium 92 Science and Technology", edited by F. H. Froes and I. R. Caplan (TMS, Pennsylvania, 1993) pp. 659–666.
3. C. M. WARD-CLOSE, P. G. PARTRIDGE and C. J. GILMORE, in "Titanium 92 Science and Technology", edited by F. H. Froes and I. R. Caplan (TMS, 1993) pp. 651–658
4. G. LU, P. G. PARTRIDGE and J. W. STEEDS, No. 2 Progress Report, IAC, University of Bristol, 1993.
5. C. M. WARD-CLOSE, G. LU and P. G. PARTRIDGE, *Mater. Sci. Eng.* (1995) In press.
6. P. B. HIRSCH, A. HOWIE, R. B. NICHOLSON, D. W. PASHLEY and M. J. WHELAN, "Electron Microscopy of Thin Crystals" (Butterworths, London, 1967).

Received 14 June
and accepted 17 July 1995